

Local oscillator phase noise limitation on the resolution of acoustic delay line wireless passive sensor measurement

N. Chrétien,¹ J.-M Friedt,^{1, a)} and G. Martin²

¹⁾*SENSeOR SAS, Besançon, France*

²⁾*FEMTO-ST, Time & frequency department, UMR CNRS 6174,
Univ. Franche Comté, Besançon, France*

(Dated: 19 March 2014)

The role of the phase noise of a local oscillator driving a pulsed-mode RADAR used for probing surface acoustic wave sensors is investigated. The echo delay, representative of the acoustic velocity and hence the physical quantity probed by the sensor, is finely measured as a phase. Considering that the intrinsic oscillator phase fluctuation defines the phase noise measurement resolution, we experimentally and theoretically assess the relation between phase noise, measurement range and measurand resolution.

PACS numbers: 84.40.-x, 43.20.Ye, 43.38.Rh

Keywords: phase noise, wireless, battery-less, surface acoustic wave, delay line, RADAR

^{a)}Electronic mail: jmfriedt@femto-st.fr; <http://jmfriedt.free.fr>

I. INTRODUCTION

Acoustic transducers have been demonstrated as suitable cooperative targets to RADAR measurements^{17,18}, hence acting as passive sensors interrogated through a wireless link. Whether implemented as the classical reflective delay line¹⁹ or the high-overtone bulk acoustic resonator¹³, a time of flight measurement always ends up as a phase measurement of the signal returned by the sensor with respect to the local oscillator.

Phase noise²⁰ is a central characteristics provided by the time and frequency analysis community when characterizing an oscillator: it defines the phase fluctuation as a function of the frequency offset from the carrier, or in other words the phase fluctuation over a duration equal to the inverse to the frequency offset from the carrier. Having demonstrated the wireless interrogation of acoustic delay lines either using a stroboscopic pulsed approach¹¹ or a wideband pulsed approach¹⁴, we here investigate how the performance of the local oscillator actually affects the physical quantity measurement resolution¹⁵. Although further processing might improve the physical quantity estimate¹⁶, the raw input remains the core limiting factor of the measurement resolution.

Even though delay line characterization is an intrinsically wideband operation, the central frequency of the emitted pulse defines the characteristics of the acoustic wave generated following the electromechanical conversion brought the piezoelectric effect. Since the distance over which the acoustic wave propagates is expressed in terms of wavelength, any change in operating frequency will affect the phase measurement: the effect of Doppler shift when interrogating a moving target will be considered as well, and the magnitude of this deterministic contribution will be compared to the random phase fluctuation characterized by phase noise.

II. DELAY LINE MEASUREMENT STRATEGIES

Acoustic delay line sensors are based on the conversion, through piezoelectricity, of an incoming electromagnetic wave to a mechanical wave whose velocity is dependent on a given physical quantity to be measured. This velocity is observed, in the wideband embodiment of the sensor configuration of the delay line, as a time of flight, which is measured as a phase between a freely running local oscillator and the carrier of the propagating electromagnetic

pulses returned as echoes from the delay line sensor.

[FIG. 1 about here.]

Although in sensing applications, two echo delay measurements are needed for a differential approach for getting rid of the distance between interrogation unit and sensor effect on the time delay measurement, we will here consider delay representative of absolute phase measurements in the 1-5 μs range (Fig. 2). Extending our considerations to the differential approach is a matter of replacing the time of flight of the pulse τ with the time of flight interval between two echoes. All experimental results were obtained using a 2.45 GHz delay line acquired from CTR (Villach, Austria) propagating a Rayleigh wave on 128 $^\circ$ -rotated cut lithium niobate.

[FIG. 2 about here.]

III. NOISE BUDGET ASSESSMENT

A physical quantity measurement based on a delay line probing requires the measurement of a time of flight which is classically performed as an accurate phase measurement following a rough counting of 2π phase rotations. This precise phase measurement is performed as a mixing between the signal returned by the delay line, with a local oscillator value at time t , and the local oscillator signal at time $t + \tau$ with τ the time needed for the electromagnetic wave to reach the sensor and the time needed for the acoustic wave to travel on the piezoelectric substrate. The former component is negligible under most circumstances. Assuming the noise stationarity, the time of the emission t is not considered and only the delay τ is accounted for in the analysis. Classical phase noise characterization of oscillators is performed by mixing the device under test with a reference oscillator exhibiting a better phase noise characteristics than the former device, and displaying the Fourier transform of the low-passed mixer output: the frequency axis of the resulting graph is the inverse of the time τ considered earlier (Fig. 3).

Two sources of phase fluctuation are considered: random fluctuations characterized as phase noise of the local oscillator, and the deterministic motion of the sensor located on a moving target which induces a Doppler shift and hence a frequency variation observed as

a phase variation through the frequency-phase slope representative of the acoustic velocity and sensor geometry. Let us consider the first component in the following analysis.

A. Random phase fluctuations

At a large enough distance, the receiver Low Noise Amplifier (LNA) phase noise dominates the local oscillator phase noise and the measurement uncertainty increases with increasing interrogation distance since the returned power decreases¹⁴. At short range, as is applicable in a multitude of industrial environments in which the sensor is confined close to the antenna linked to the interrogation unit (e.g. motor rotor to stator distance), the local oscillator phase noise dominates. Its contribution is dependent on the local oscillator noise floor b_0 and the emitted power P_E : the range d beyond which the LNA dominates over the oscillator phase noise is¹⁴

$$d = \frac{\lambda}{4\pi} \sqrt[4]{\frac{P_E \cdot b_0}{k_B \cdot T \cdot IL}}$$

which, at 2.45 GHz (*i.e.* an electromagnetic wavelength $\lambda = 12.5$ cm), for a noise floor of the local oscillator $b_0 = -100$ dBc/Hz, an emitted power of 10 dBm and an insertion loss of the sensor $IL = 40$ dB, is equal to 12 cm (with $k_B \cdot T$ the Boltzmann constant times the temperature being the classical -174 dBm/Hz constant at ambient).

Typical acoustic delays lie in the 1 to 5 μ s range, the lower value being defined by the rejection of clutter and switching time of radiofrequency electronics in a monostatic RADAR configuration, and the upper bound by the acoustic delay line dimensions and associated acoustic propagation losses. Furthermore, state of the art ultra-high frequency (UHF) oscillators exhibit a Leeson frequency around 100 kHz associated with a time delay of 10 μ s: keeping the maximum delay at 5 μ s safely keeps all considerations within the phase noise plateau, beyond the flicker noise region.

[FIG. 3 about here.]

B. Doppler shift related phase fluctuations

Consider a delay line located on a moving target such as a wheel of a vehicle driving at 250 km/h: the velocity of the sensor v with respect to the interrogation unit antenna located on the vehicle ranges from -250 to 250 km/h. The associated Doppler frequency shift Δf_D

when the delay line is probed at a central frequency $f_0 = 2450$ MHz is approximated as $\Delta f_D = 2f_0 \cdot v/c_0$ with c_0 the speed of an electromagnetic wave in vacuum, since $v \ll c_0$. This amounts to $\Delta f_D \in [\pm 1130]$ Hz. This frequency fluctuation is considered randomly distributed in this interval since the sensor measurement time is incoherent with the wheel motion, and hence the resulting phase noise is analyzed in the context of a white noise contribution. This central frequency variation affects the phase measurement since both quantities are related by the wavelength of the acoustic wave propagating on the piezoelectric substrate: since one wavelength path length accounts for a 2π phase rotation, the total phase fluctuation when the acoustic wave propagates a distance D is $\varphi = 2\pi D/\lambda = 2\pi D f_0/v_a = 2\pi\tau f_0$ with v_a the acoustic wave velocity on the piezoelectric substrate and τ the two-way trip acoustic pulse delay. Hence, any change in f_0 due to the Doppler shift is detected as a $\Delta\varphi$ phase variation: $\Delta\varphi = 2\pi\tau\Delta f_0$. Since $\tau < 3 \mu\text{s}$, the ± 1130 Hz variation yields $|\Delta\varphi| < 0.02$ rad. Assuming a measurement bandwidth $B = 30$ MHz, such a phase variation is equivalent to a local oscillation phase noise of $S_\varphi = \Delta\varphi^2/B = 1.5 \cdot 10^{-11}$ rad²/Hz or -110 dBrad²/Hz.

From such considerations, the use of a local oscillator exhibiting a noise floor better than -110 dBrad²/Hz is irrelevant for probing fast-moving acoustic delay lines since the Doppler shift is the dominant phase fluctuation factor.

IV. PHYSICAL QUANTITY MEASUREMENT

The final consideration lies in the conversion from phase measurement to a physical quantity. We focus on a temperature measurement but the consideration is valid for any physical quantity locally linearly dependent with the phase (first order expansion). Since the phase is representative of the velocity of the acoustic wave (assuming a fixed length of the propagation path), then

$$\frac{\partial\varphi(T)}{\varphi} = \frac{\partial v_a(T)}{v_a} \Leftrightarrow \partial\varphi(T) = \varphi \times \frac{\partial v_a(T)}{v_a} = 2\pi f_0\tau \frac{\partial v_a(T)}{v_a}$$

This quantity providing the phase variation for a unit temperature variation is defined as the temperature sensitivity s of the device, dependent on the material properties of the piezoelectric substrate, the geometry and the operating frequency. In the case of the classical lithium niobate substrate used for delay line manufacturing, $v_a = 4000$ m/s and its temperature sensitivity $\partial v_a(T)/v_a$ is 60 ppm/K.

[FIG. 4 about here.]

Table I summarizes the temperature sensitivity s (rad/K) for various sensor geometries and operating frequencies, as well as the temperature measurement resolution assuming oscillator phase noise plateau of -90 dBc/Hz (T_{-90}) and -130 dBc/Hz (T_{-130}) deduced by considering that the local oscillator phase noise b_0 is defined as the phase fluctuation standard deviation σ_φ integrated over the measurement bandwidth B : $\sigma_\varphi = \sqrt{b_0 \times B}$. Such a random phase fluctuation prevents the use of this quantity to extract the physical measurement below a σ_φ/s resolution, which is computed in the two right columns of Tab. I. In all cases the measurement bandwidth was considered as $B = 50$ MHz. The 100 MHz case relates to the devices depicted in¹², in which the local oscillator is not embedded in the probing signal source but in the receiving clocking circuit.

[TABLE 1 about here.]

A practical validation of these considerations is depicted in Fig. 5, in which the phase fluctuation measurements displayed in Fig. 4 are converted to temperature measurement resolutions. Three frequency sources operating at 2.45 GHz are considered: a Marconi 2042 signal generator, an Agilent E5071B network analyzer with a frequency span set to 0-Hz, and a Marconi 2042 whose output is attenuated by 39 dB to rise the noise floor ($-174 + 39 = -135$ dBrad²/Hz noise floor after attenuation of the 0 dBm output) before amplification to compensate for the losses of the attenuators and generate a +1 dBm output (the resulting source being referenced to as “degraded Marconi” in the figures). Notice that even though the phase noise rises with increasing pulse echo delay (as expected from local oscillator detuning with time delay), the temperature resolution increases as a function of delay since the phase rotations due to the propagating acoustic delay line rises faster than the associated noise level since the phase noise plateau has already been reached. The most accurate temperature resolution prediction from Fig. 5 might not be reached experimentally due to insufficient thermal stabilization during the data acquisition.

[FIG. 5 about here.]

Other sources of noise in the phase measurement include the analog to digital conversion (ADC) step, and most significantly the quantization error on the one hand, and jitter on the

ADC clock on the other hand. The latter effect is negligible considering the long (20 to 30 ns long for 50 to 30 MHz bandwidth) pulses needed to probe the delay line response. Typical phase jitters of the clock triggering the ADC are in the sub-nanosecond range, given by σ_φ/f_0 the ratio of the clocking circuit phase noise to clocking frequency ratio. A -100 dBrad²/Hz clock operating at 100 MHz would generate a clock jitter of 0.7 ns, or much less than the pulse duration.

ADC quantification is estimated in the case of this experiment by considering that the quantization noise $V_q^2/12$ with V_q the quantization voltage is distributed over the whole measurement bandwidth. The LeCroy WaveRunner LT374M oscilloscope used to acquire the data presented in the phase resolution estimates quanticizes on a 8 bit scale and a $B = 2$ GHz bandwidth: the quantization noise floor is $V_q^2/(12 \cdot B)$ or less than -150 dBrad²/Hz, again much less than all the other noise sources considered so far.

Finally, the intrinsic phase noise of the Hittite HMC597LP4 I/Q demodulator is not relevant to this experiment since with a noise factor of 15 dB and a local oscillator input power of 0 dBm, the noise floor of -159 dBrad²/Hz is again below the local oscillator and low noise amplifier noise floors.

V. CONCLUSION

An error budget analysis for a pulsed mode interrogation system for probing acoustic delay lines acting as passive, wireless sensor is proposed based on phase noise analysis. At short range the short term local oscillator stability is the limiting factor considering a typical, off the shelf device exhibiting a noise floor in the -130 dBrad²/Hz in the 0.2-1 MHz offset from the carrier frequencies. At long range, the receiver low noise amplifier thermal noise becomes dominant: the intrinsic wideband nature of the acoustic delay line transfer function requires a broadband first receiver stage which necessarily induces large phase fluctuation at the mixer input when the received power becomes low enough (i.e. at some distance the receiver noise level rises above the local oscillator noise floor).

REFERENCES

- ¹N. Chrétien, J.-M. Friedt, G. Martin, and S. Ballandras. A stroboscopic approach to surface acoustic wave delay line interrogation. In *Joint European Frequency and Time Forum and IEEE International Frequency Control Symposium*, pages 771–774, Prague, Czech Rep., 2013.
- ²J.-M. Friedt, T. Rétonnaz, S. Alzuaga, T. Baron, G. Martin, T. Laroche, S. Ballandras, M. Griselin, and J.-P. Simonnet. Surface acoustic wave devices as passive buried sensors. *Journal of Applied Physics*, 109(3):034905, 2011.
- ³J.-M. Friedt, A. Saintenoy, S. Chrétien, T. Baron, É. Lebrasseur, T. Laroche, S. Ballandras, and M. Griselin. High-overtone bulk acoustic resonator as passive ground penetrating RADAR cooperative targets. *J. Appl. Phys.*, 113(13):134904, 2013.
- ⁴G. Goavec-Mérou, N. Chrétien, J.-M. Friedt, P. Sandoz, G. Martin, M. Lenczner, and S. Ballandras. Fast contactless vibrating structure characterization using real time field programmable gate array-based digital signal processing: Demonstrations with a passive wireless acoustic delay line probe and vision. *Rev. Sci. Instrum.*, 85(1):015109, Jan. 2014.
- ⁵V. Kalinin. Influence of receiver noise properties on resolution of passive wireless resonant SAW sensors. In *IEEE Int. Ultrasonics Symposium*, pages 1452–1455, Rotterdam, Holland, 19-21 Sep. 2005.
- ⁶V. Kalinin, B. Dixon, and J. Beckley. Optimization of resonant frequency measurement algorithm for wireless passive SAW sensors. In *Joint 22nd European Frequency and Time forum and IEEE International Frequency Control Symposium*, pages 90–95, 2009.
- ⁷J. H. Kuypers, L. M. Reindl, S. Tanaka, and M. Esashi. Maximum accuracy evaluation scheme for wireless SAW delay-line sensors. *IEEE Transactions on ultrasonics, ferroelectrics, and frequency control*, 55(7), July 2008.
- ⁸J. H. Kuypers, S. Tanaka, M. Esashi, D. A. Eisele, and L. M. Reindl. Passive 2.45 GHz TDMA based multi-sensor wireless temperature monitoring system: Results and design considerations. In *IEEE Ultrasonics Symposium*, pages 1453–1458, 2006.
- ⁹V.P. Plessky and L.M. Reindl. Review on SAW RFID tags. *IEEE Trans Ultrason Ferroelectr Freq Control*, 57(3):654–668, Mar 2010.
- ¹⁰E. Rubiola. *Phase Noise and Frequency Stability in Oscillators*. Cambridge University Press, 2010.

- ¹¹N. Chrétien, J.-M. Friedt, G. Martin, and S. Ballandras. A stroboscopic approach to surface acoustic wave delay line interrogation. In *Joint European Frequency and Time Forum and IEEE International Frequency Control Symposium*, pages 771–774, Prague, Czech Rep., 2013.
- ¹²J.-M Friedt, T. Rétonnaz, S. Alzuaga, T. Baron, G. Martin, T. Laroche, S. Ballandras, M. Griselin, and J.-P. Simonnet. Surface acoustic wave devices as passive buried sensors. *Journal of Applied Physics*, 109(3):034905, 2011.
- ¹³J.-M Friedt, A. Saintenoy, S. Chrétien, T. Baron, É. Lebrasseur, T. Laroche, S. Ballandras, and M. Griselin. High-overtone bulk acoustic resonator as passive ground penetrating RADAR cooperative targets. *J. Appl. Phys.*, 113(13):134904, 2013.
- ¹⁴G. Goavec-Mérou, N. Chrétien, J.-M Friedt, P. Sandoz, G. Martin, M. Lenczner, and S. Ballandras. Fast contactless vibrating structure characterization using real time field programmable gate array-based digital signal processing: Demonstrations with a passive wireless acoustic delay line probe and vision. *Rev. Sci. Instrum*, 85(1):015109, Jan. 2014.
- ¹⁵V. Kalinin. Influence of receiver noise properties on resolution of passive wireless resonant SAW sensors. In *IEEE Int. Ultrasonics Symposium*, pages 1452–1455, Rotterdam, Holland, 19-21 Sep. 2005.
- ¹⁶V. Kalinin, B. Dixon, and J. Beckley. Optimization of resonant frequency measurement algorithm for wireless passive SAW sensors. In *Joint 22nd European Frequency and Time forum and IEEE International Frequency Control Symposium*, pages 90–95, 2009.
- ¹⁷J. H. Kuypers, L. M. Reindl, S. Tanaka, and M. Esashi. Maximum accuracy evaluation scheme for wireless SAW delay-line sensors. *IEEE Transactions on ultrasonics, ferro-electrics, and frequency control*, 55(7), July 2008.
- ¹⁸J. H. Kuypers, S. Tanaka, M. Esashi, D. A. Eisele, and L. M. Reindl. Passive 2.45 GHz TDMA based multi-sensor wireless temperature monitoring system: Results and design considerations. In *IEEE Ultrasonics Symposium*, pages 1453–1458, 2006.
- ¹⁹V.P. Plessky and L.M. Reindl. Review on SAW RFID tags. *IEEE Trans Ultrason Ferro-electric Freq Control*, 57(3):654–668, Mar 2010.
- ²⁰E. Rubiola. *Phase Noise and Frequency Stability in Oscillators*. Cambridge University Press, 2010.

LIST OF FIGURES

1	Basics of a pulsed-mode SAW delay line acoustic sensor interrogation scheme emphasizing the influence of the local oscillator phase noise. The source at a fixed frequency ν is gated at time t and the signal returns after a time τ including the electromagnetic and acoustic propagation durations. Throughout the discussion, the offset from the carrier $f = 1/\tau$ is considered. The component references are those used to demonstrate experimentally the concepts developed in this paper.	11
2	I and Q component measurements of an acoustic delay line probed by various radiofrequency sources characterized by different phase noise distributions. Although the contribution of the phase noise is hardly visible on these raw data, the emphasis is on the operation at constant received power for all tester radiofrequency sources.	12
3	Phase noise of the sources considered in this document for probing a 2450 MHz acoustic delay line acting as passive sensor. Although the Agilent source significantly fluctuates around the frequency offset from carrier of interest, the phase noise value of -127 dBrad ² /Hz was selected to best match experimental results.	13
4	Phase measurement standard deviation as a function of the echo delay. The 3 dB rise with respect to the raw oscillator phase noise measurement is associated with adding the noise contributions of the two inputs during the mixing process.	14
5	Conversion from phase noise to temperature measurement, considering a 2 GHz measurement bandwidth (4 GS/s digital oscilloscope records): notice that the rising phase noise with delay is compensated for by the rising sensitivity with increasing delay. The dashed lines indicate the expected temperature measurement standard deviation for nominal phase noise values plus or minus 1 dBrad ² /Hz and hence act as error bars.	15

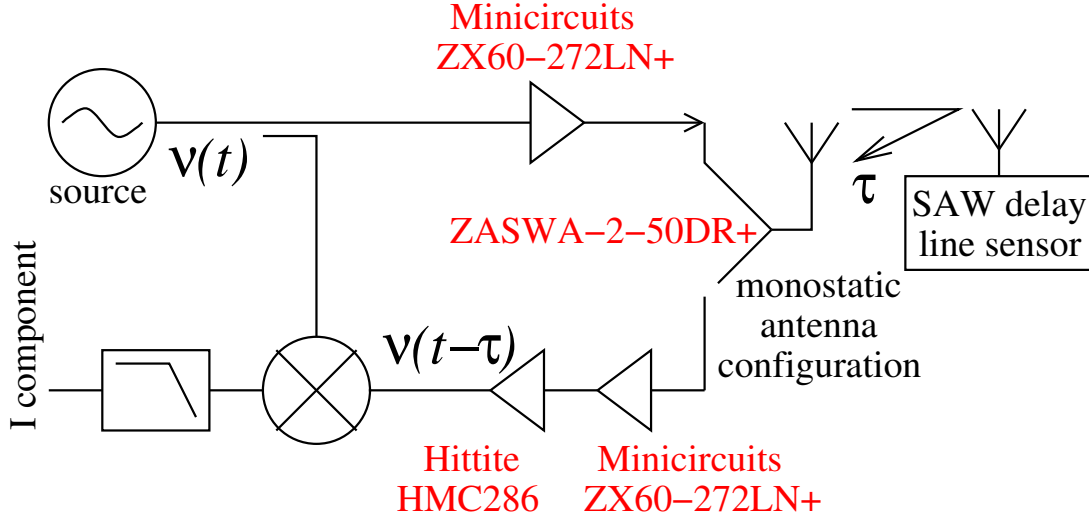


FIG. 1. Basics of a pulsed-mode SAW delay line acoustic sensor interrogation scheme emphasizing the influence of the local oscillator phase noise. The source at a fixed frequency ν is gated at time t and the signal returns after a time τ including the electromagnetic and acoustic propagation durations. Throughout the discussion, the offset from the carrier $f = 1/\tau$ is considered. The component references are those used to demonstrate experimentally the concepts developed in this paper.

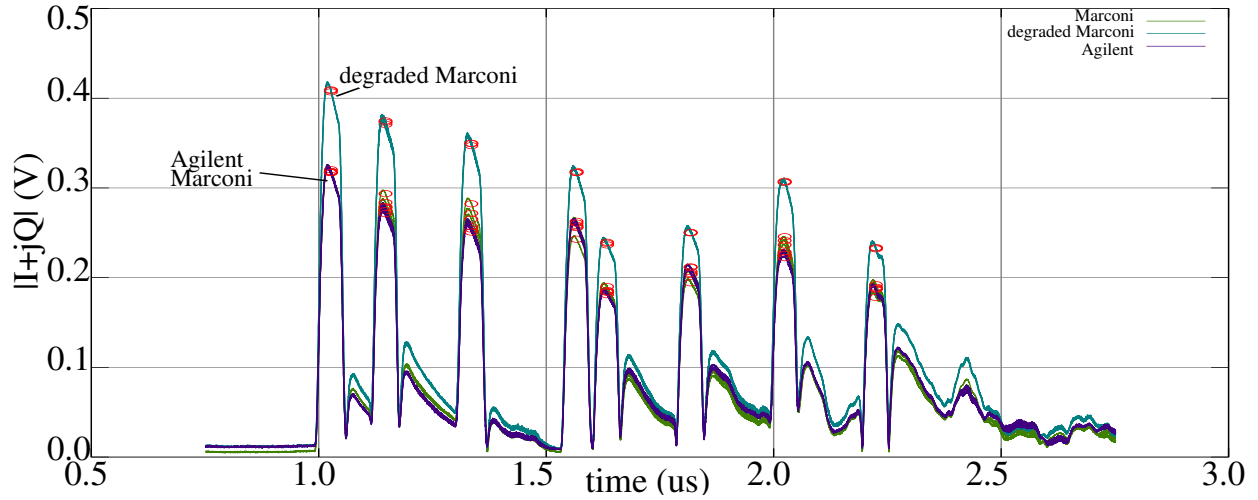


FIG. 2. I and Q component measurements of an acoustic delay line probed by various radiofrequency sources characterized by different phase noise distributions. Although the contribution of the phase noise is hardly visible on these raw data, the emphasis is on the operation at constant received power for all tester radiofrequency sources.

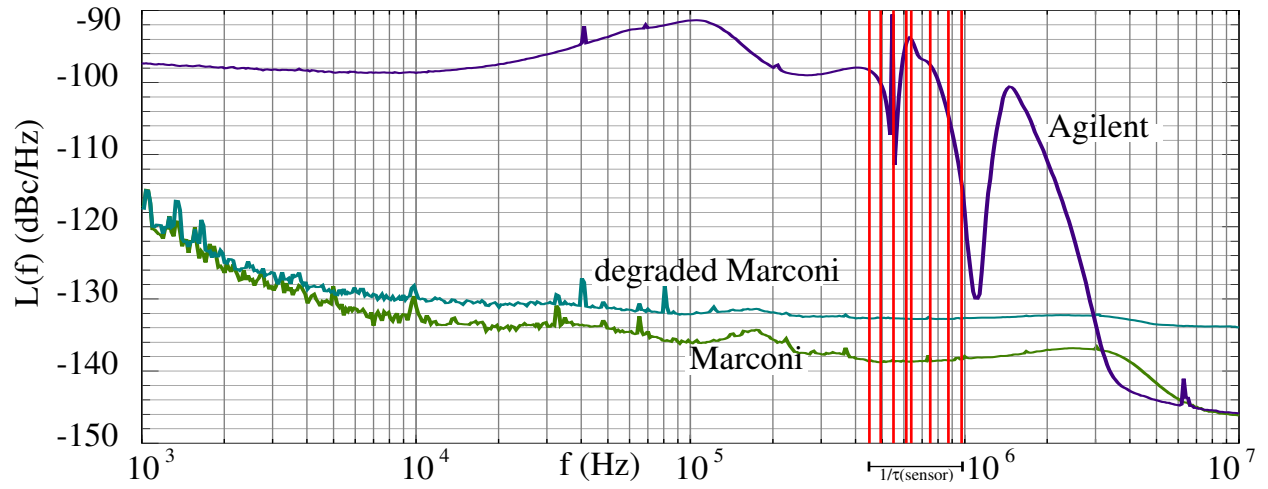


FIG. 3. Phase noise of the sources considered in this document for probing a 2450 MHz acoustic delay line acting as passive sensor. Although the Agilent source significantly fluctuates around the frequency offset from carrier of interest, the phase noise value of $-127 \text{ dBc}^2/\text{Hz}$ was selected to best match experimental results.

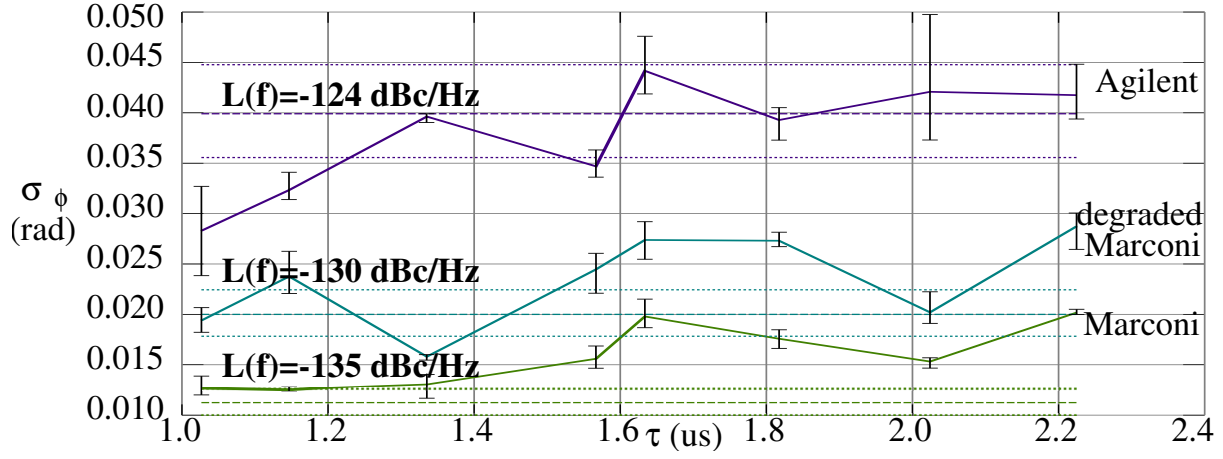


FIG. 4. Phase measurement standard deviation as a function of the echo delay. The 3 dB rise with respect to the raw oscillator phase noise measurement is associated with adding the noise contributions of the two inputs during the mixing process.

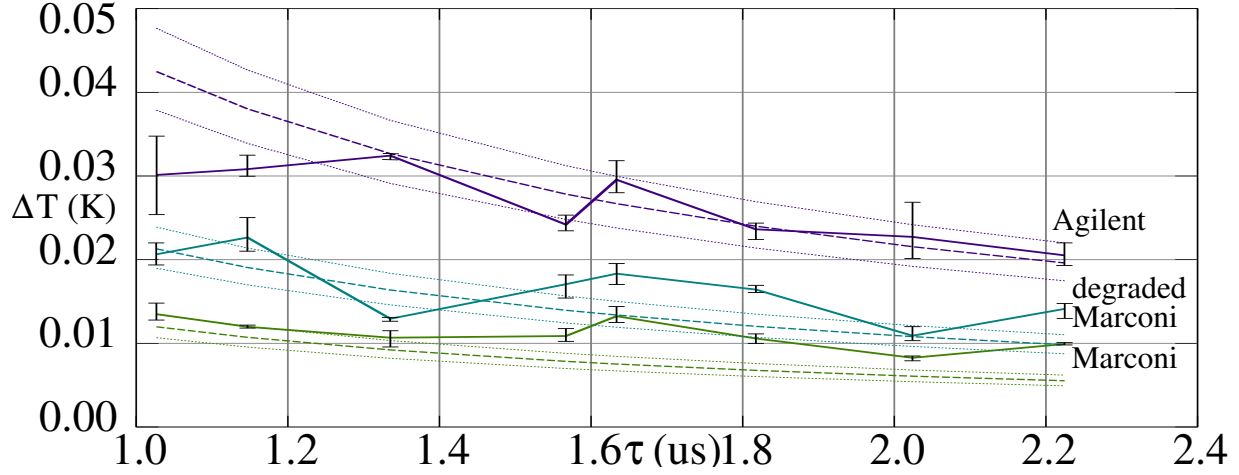


FIG. 5. Conversion from phase noise to temperature measurement, considering a 2 GHz measurement bandwidth (4 GS/s digital oscilloscope records): notice that the rising phase noise with delay is compensated for by the rising sensitivity with increasing delay. The dashed lines indicate the expected temperature measurement standard deviation for nominal phase noise values plus or minus 1 dBrad²/Hz and hence act as error bars.

LIST OF TABLES

I	Influence of local oscillator phase noise and sensor geometry on the measurement resolution. The single sideband phase noise $L(f)$ is related to the phase noise S_φ by a factor of 2 during the numerical application.	17
---	---	----

TABLE I. Influence of local oscillator phase noise and sensor geometry on the measurement resolution. The single sideband phase noise $L(f)$ is related to the phase noise S_φ by a factor of 2 during the numerical application.

f (MHz)	τ (μ s)	s (rad/K)	T_{-90} (K)	T_{-130} (K)
100	1	0.038	8.4	$8 \cdot 10^{-2}$
100	3	0.113	2.8	$3 \cdot 10^{-2}$
2450	1	0.924	0.34	$3 \cdot 10^{-3}$
2450	3	2.77	0.11	$1 \cdot 10^{-2}$